JACS JOURNAL OF THE AMERICAN CHEMICAL SOCIETY

COMMUNICATION

pubs.acs.org/JACS

A Three-State Surface-Confined Molecular Switch with Multiple Channel Outputs

Cláudia Simão, Marta Mas-Torrent,* Javier Casado-Montenegro, Francisco Otón, Jaume Veciana, and Concepció Rovira*

Institut de Ciència de Materials de Barcelona (ICMAB-CSIC) and Networking Research Center on Bioengineering, Biomaterials and Nanomedicine (CIBER-BBN), Campus de la UAB, 08193 Bellaterra, Spain

Supporting Information

ABSTRACT: A self-assembled monolayer of a tetrathiafulvalene derivative on indium tin oxide is shown to operate as a ternary redox switch in which the magnetic and optical outputs are employed to provide a readout of the state. This surface-confined molecular switch exhibits excellent reversibility and stability and is thus promising for the development of molecular electronics.

An increasing interest in grafting functional organic molecules onto solid supports is emerging, motivated by the fabrication of molecular-controlled electronic devices as an alternative to the miniaturization limitations faced by established silicon-based microelectronics. Additionally, such organic/inorganic hybrids can give rise to new materials with unprecedented performance. In these directions, bistable molecules are particularly appealing for their potential to serve as active components in data-storage devices.[1] Such bistability can stem from intramolecular electron-transfer processes, acid/base pairs, distinct magnetic interactions, isomerization transformations, or redox reactions. Mostly these latter two origins of bistability have been exploited in surface-confined molecules using light or electrical inputs to trigger the transformations. Molecular switches consisting of self-assembled monolayers (SAMs) of photo- or electrochromic molecules as well as molecules that change their electrical behavior upon photoisomerization have been reported previously.[2−11] Also, surfaces functionalized with multifunctional organic radicals have been described very recently,[12−14] and their potential as robust platforms for nonvolatile memory devices with optical and magnetic responses has been demonstrated.[15] Since all of these molecular switches are based on two states (i.e., ON and OFF states), they offer great potential for use in binary logic gates.[16,17] The fabrication of devices with surface-confined molecules that can be reversibly interconverted between three stable states is very rare,[18,19] although it would allow for the execution of more complex logic operations and also increase further the data storage capacity by going from 2^n memory units in a binary system to 3^n in a ternary one.

Tetrathiafulvalenes (TTFs) have been studied for many years for their fascinating electrical properties and remarkable electrochemical behavior.[20−25] TTF SAMs have also been explored, primarily to investigate their electrochemical properties and in the development of ion sensors.[26−32] These molecules exhibit in solution three stable and accessible redox states (i.e., neutral, radical cation, and dication states) and therefore can act as key building blocks in switchable redox processes when grafted on conducting surfaces.[33] Here we report on the excellent switching properties of novel TTF SAMs on indium tin oxide (ITO) substrates that employ an electrochemical input and use optical and magnetic outputs as readout signals. The high potential of these systems for use as ternary memory devices is clearly elucidated.

Scheme 1. Synthetic Route for Preparation of 1

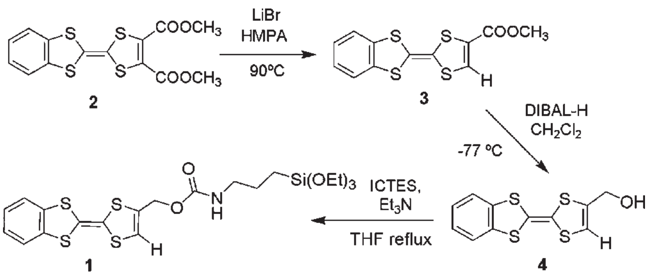

TTF derivative **1** was employed to functionalize ITO, a transparent conducting substrate (Scheme 1). This molecule was designed with a terminated triethoxysilane moiety as a surface-anchoring group and a benzene ring to further promote lateral $\pi-\pi$ interactions between TTFs as well as an amide bridging group that could favor H-bonding among the neighboring grafted molecules. Therefore, this molecular design can drive dense molecular packing. To synthesize the target TTF molecule, monodecarboxylation of the asymmetric 4,5-dicarboxymethoxybenzotetrathiafulvalene **2**[34−37] was first carried out using lithium bromide in hexamethylphosphoramide (HMPA) at 90 °C in high yield (92%). The conversion of ester **3** to primary alcohol **4** was achieved by reduction with diisobutylaluminum hydride (DIBAL-H) at low temperature (61% yield). Finally, the condensation reaction of **4** with 3-isocyanatopropyltriethoxysilane (ICTES) and triethylamine in refluxing THF afforded the desired TTF silane derivative **1** (30% yield).

SAMs of **1** on ITO-coated glass were fabricated by immersion of the freshly cleaned substrates in a 1 mM solution of **1** in dry toluene under an inert atmosphere. The solution was kept in a thermostatted oil bath at 80 °C for the first 3 h and then left at room temperature overnight. Afterward, the functionalized substrates were rinsed thoroughly with toluene and dried under a

Received: May 27, 2011
Published: August 02, 2011

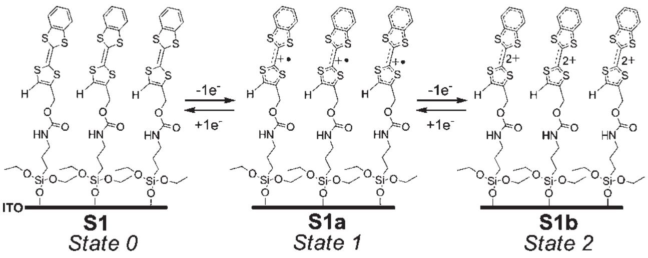

Figure 1. Schematic representation of the electrochemical tristability of SAM **S1** obtained from **1**.

stream of nitrogen, giving SAM **S1** (Figure 1), which was fully characterized by contact angle (CA) measurements, X-ray photoelectron spectroscopy (XPS), and time-of-flight secondary-ion mass spectrometry (TOF−SIMS). The higher CA of 74.1° for **S1** relative to that of bare ITO (51.2°) was in agreement with the hydrophobic nature of the terminal benzene rings,[38,39] confirming the successful surface functionalization. The XPS spectra showed the appearance of S and Si elements along with an increasing amount of carbon (S 2p, 163.21 eV; Si 2p, 102.22 eV; C 1s, 296.20 eV). In the TOF−SIMS spectrum, the molecular peak appeared at m/z 426, pointing out the loss of two ethoxy groups from the silane moiety [Figure S1 in the Supporting Information (SI)].

The electrochemical characteristics of SAM **S1** were investigated using cyclic voltammetry (CV). The experiments were carried out in a 0.02 M solution of tetrabutylammonium hexafluorophosphate (TBAHFP) in acetonitrile using the functionalized substrate as the working electrode [vs Ag(s)]. As shown in Figure 2a, the cyclic voltammogram exhibited two reversible redox waves. The first, at $E^{(1)}_{1/2}$ = +0.74 V, was assigned to the oxidation forming the radical cation species (**S1a** in Figure 1), and the second one, at $\mathrm{E}^{(2)}_{1/2}$ = +1.30 V with a higher current density but equal integration, was attributed to the oxidation to the dication (**S1b** in Figure 1). Such an asymmetric cyclic voltammogram shape is typical of dense TTF SAMs on Au and has previously been explained in terms of intermolecular electron interactions taking place within the monolayer.[26,32,40] The surface coverage (Γ) of the SAM was estimated from the anodic charge integration at 100 mV/s to have the high value of 1.1 × 10^{-10} mol/cm^2 (87% coverage; see the SI). It was also observed that the current peaks increased with the scan rate, which is characteristic of surface-confined electroactive species. The stabilities of the three redox states were confirmed by performing many consecutive voltage cycles from 0 to +1.5 V, which resulted in completely identical redox waves that did not show any sign of loss of current intensity (Figure 2b).

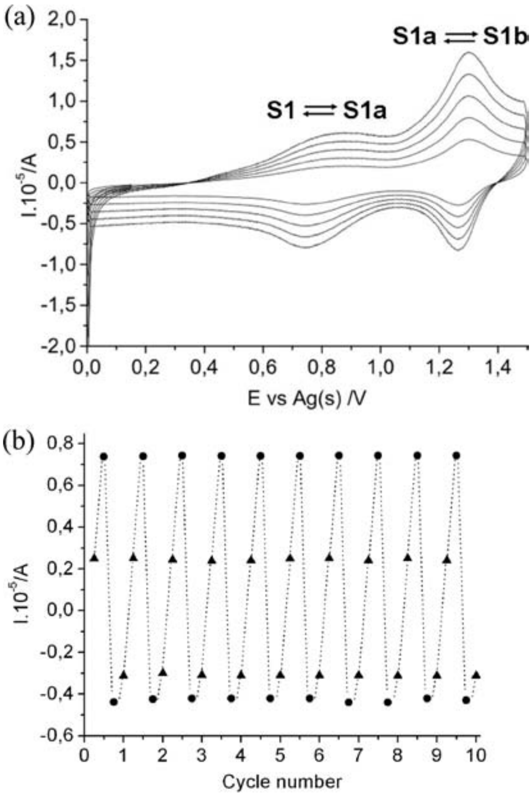

Figure 2. (a) CV response using the SAM of **1** as the working electrode vs Ag(s) and a Pt wire as the counter electrode in 0.02 M TBAHFP in acetonitrile. The different cycles correspond to scan rates of (from lower to higher current intensity) 0.05, 0.1, 0.15, 0.2, and 0.25 V/s. (b) Plot of the current intensity vs the number of cycles of the two redox peaks corresponding to the processes **S1** ⇄ **S1a** (▲) and **S1a** ⇄ **S1b** (●) at scan rate of 0.1 V/s.

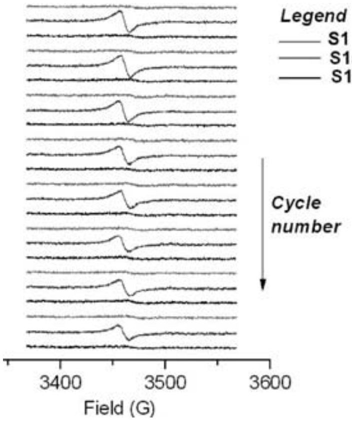

Figure 3. Magnetic response of the SAM of **1** monitored by EPR spectroscopy when a sequence of consecutive voltage pulses of −0.2, +0.9, and +1.5 V vs Ag(s) were applied to the substrate.

Since the radical cation species formed after the first oxidation process confers paramagnetic properties to the SAM, the magnetic response of the three redox states was employed as a readout signal of the electrochemical switch by monitoring the electronic paramagnetic resonance (EPR) spectrum. After the appropriate voltage was applied to **S1** for 2 min in the CV cell, the EPR spectrum of the SAM was registered in air. A sequence of voltage pulses of −0.2, +0.9, and +1.5 V vs Ag(s) was applied in order to convert the SAM to **S1** (state 0), **S1a** (state 1), and **S1b** (state 2), respectively. The collected EPR spectra are shown in Figure 3. Flat EPR baselines were observed for the neutral (**S1**) and dicationic (**S1b**) states in accord with their diamagnetic character, whereas for the radical cation state (**S1a**), a broad line (ΔH_{pp}= 10 G) at a g factor of 2.0082 was seen, as is typical for solid-state TTF$^{+\bullet}$.[20,22] Importantly, the same spectra could be reproduced after several weeks. This result confirmed unambiguously the viability of using the magnetic response to read the state of the switch.

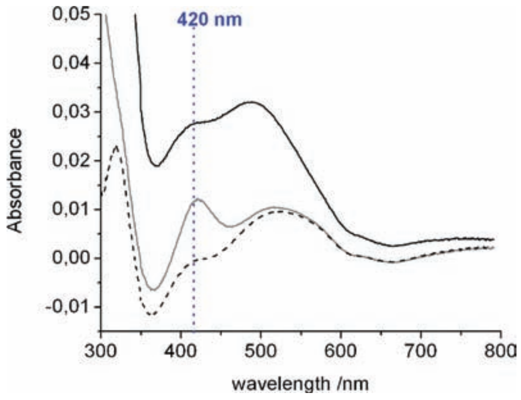

Figure 4. UV−vis absorbance spectra of **S1** (black dashed line), **S1a** (gray solid line), and **S1b** (black solid line) in a solution of 20 mM TBAHFP in acetonitrile. **S1a** and **S1b** were generated applying voltages of +0.9 and +1.5 V vs Ag(s), respectively, for 2 min. The vertical dashed line indicates the wavelength that was monitored in the switching studies.

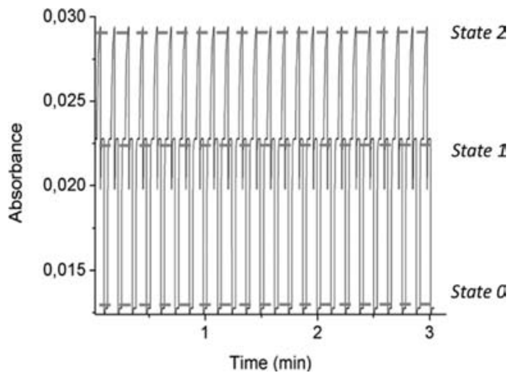

Figure 5. Optical absorbance of the SAM of **1** at λ = 420 nm as a function of time upon consecutive application of a sequence of 2 s pulses at voltages vs Ag(s) of −0.2 V (state 0), +0.9 V (state 1), and +1.5 V (state 2).

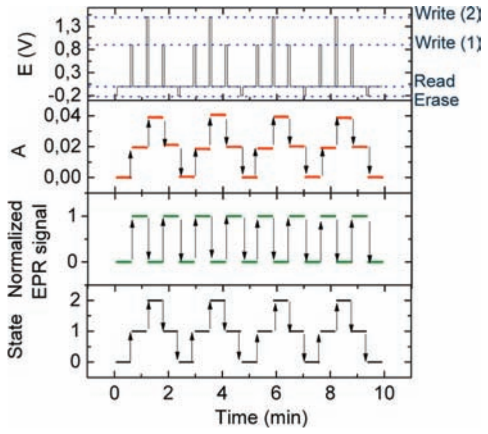

Figure 6. Three-state switching behavior of the SAM of **1**: (top to bottom) applied voltage profile, optical output (absorbance at 420 nm), magnetic output (EPR signal), and corresponding states (0, 1, and 2).

The optical response of the SAM was also explored to interrogate the switch. SAM **S1** was placed in a UV−vis cuvette filled with a 0.02 M solution of TBAHFP as the electrolyte in acetonitrile. Platinum and silver wires were employed as the counter and reference electrodes, respectively, to perform electrochemistry in situ in the UV−vis spectrophotometer. Figure 4 shows the UV−vis spectra of the three redox states of the SAM, which were achieved applying the same voltages as in the previously described experiments. A band at 420 nm typical of a TTF radical cation was observed for **S1a**. On the other hand, upon oxidation to **S1b**, the collected UV−vis spectrum showed a notable increase in the absorbance of the functionalized substrate and the appearance of a broad band at ~500 nm. On the basis of the different absorption spectra of the three states, the electrochemical switching of these SAMs was monitored by following the absorption changes at 420 nm. For this purpose, cycles with a voltage profile involving 2 s pulses of ERASE (−0.2 V)−WRITE 1 (+0.9 V)−WRITE 2 (+1.5 V) were applied in order to commute from state 0 to state 1 and then to state 2. As shown in Figure 5, three different absorption values with high ON/OFF ratios were found to be distinguishable and characteristic of the three states, confirming that optical readout of the charge storage is feasible. Hundreds of cycles without loss of the signal recovery were performed, confirming the high stability of the three redox states of the SAM (Figures S2 and S3). Furthermore, the outstanding SAM stability over time was also confirmed, as the switching behavior was maintained for over a month (Figure S5).

In order to investigate further the potential of the TTF SAM for nonvolatile memory devices, a cyclic series of WRITE 1−READ−WRITE 2−READ−ERASE−READ voltage pulses [+0.9, 0, +1.5, 0, −0.2, 0 V vs Ag(s), respectively] were applied. The WRITE and ERASE pulses were applied for 5 s and the READ pulses for 30 s. Figure 6 summarizes the optical and magnetic outputs measured. The results clearly reveal that the three states of the switch were preserved after removal of the external electrical stimuli. Considering first the magnetic response, we observe that even if the SAM can be in three different states, only one EPR response is detectable because two of the states do not exhibit any EPR signal. In other words, the EPR output can be either ON or OFF (i.e., in binary language 1 or 0). However, three levels of optical absorbance can be identified (i.e., high for state 2, medium for state 1, and low for state 0). This points out that this system is suitable for use in both binary and ternary memory devices.

In summary, by taking advantage of the multiplicity of redox states of TTFs, their stability, and the reversibility of their interconversions when grafted on a substrate, we were able to fabricate a three-state surface-immobilized switch by exploiting their distinct optical and magnetic responses. The excellent robustness and stability of this molecular switch represents one modest but significant contribution to the great potential that molecular electronics offers for developing real devices.

■ ASSOCIATED CONTENT

Ⓢ Supporting Information. Experimental procedures and additional data. This material is available free of charge via the Internet at http://pubs.acs.org.

■ AUTHOR INFORMATION

Corresponding Authors

mmas@icmab.es; cun@icmab.es

■ ACKNOWLEDGMENT

The research leading to these results received funding from the European Community's Seventh Framework Programme (FP7/2007-2013) under Grant Agreement 212311 of the ONE-P Project; the Marie Curie Est FuMASSEC; the DGI (Spain) under Grants EMOCIONa (CTQ2006-06333) and POMAs (CTQ2010-19501); the Networking Research Center on Bioengineering, Biomaterials and Nanomedicine (CIBER-BBN); CSIC (PIF200850F0080); and Generalitat de Catalunya (Grant 2009SGR00516). We also thank Dr. Lloveras for the EPR measurements and Amable Bernabé for the MALDI measurements.

■ REFERENCES

(1) *Molecular Devices and Machines: Concepts and Perspectives for the Nanoworld*; Balzani, V.; Credi, A.; Venturi, M., Eds.; Wiley-VCH: Weinheim, Germany, 2008.

(2) Gupta, T.; Altman, M.; Shukla, A. D.; Freeman, D.; Leitus, G.; van der Boom, M. E. *Chem. Mater.* **2006**, *18*, 1379.

(3) Shukla, A. D.; Das, A.; van der Boom, M. E. *Angew. Chem., Int. Ed.* **2005**, *44*, 3237.

(4) Sortino, S.; Di Bella, S.; Conoci, S.; Petralia, S.; Tomasulo, M.; Paesial, E. J.; Raymo, F. M. *Adv. Mater.* **2005**, *17*, 1390.

(5) Sortino, S.; Petralia, S.; Conoci, S.; Di Bella, S. *J. Mater. Chem.* **2004**, *14*, 811.

(6) Areephong, J.; Browne, W. R.; Katsonis, N.; Feringa, B. L. *Chem. Commun.* **2006**, 3930.

(7) Katsonis, N.; Kudernac, T.; Walko, M.; van der Molen, S. J.; van Wees, B. J.; Feringa, B. L. *Adv. Mater.* **2006**, *18*, 1397.

(8) Kronemeijer, A. J.; Akkerman, H. B.; Kudernac, T.; van Wees, B. J.; Feringa, B. L.; Blom, P. W. M.; de Boer, B. *Adv. Mater.* **2008**, *20*, 1467.

(9) Namiki, K.; Sakamoto, A.; Murata, M.; Kume, S.; Nishihara, H. *Chem. Commun.* **2007**, 4650.

(10) Ferri, V.; Elbing, M.; Pace, G.; Dickey, M. D.; Zharnikov, M.; Samorì, P.; Mayor, M.; Rampi, M. A. *Angew. Chem., Int. Ed.* **2008**, *47*, 3407.

(11) Mativetsky, J. M.; Pace, G.; Elbing, M.; Rampi, M. A.; Mayor, M.; Samorì, P. *J. Am. Chem. Soc.* **2008**, *130*, 9192.

(12) Crivillers, N.; Mas-Torrent, M.; Perruchas, S.; Roques, N.; Vidal-Gancedo, J.; Veciana, J.; Rovira, C.; Basabe-Desmonts, L.; Ravoo, B. J.; Crego-Calama, M.; Reinhoudt, D. N. *Angew. Chem., Int. Ed.* **2007**, *46*, 2215.

(13) Crivillers, N.; Mas-Torrent, M.; Vidal-Gancedo, J.; Veciana, J.; Rovira, C. *J. Am. Chem. Soc.* **2008**, *130*, 5499.

(14) Mas-Torrent, M.; Crivillers, N.; Mugnaini, V.; Ratera, I.; Rovira, C.; Veciana, J. *J. Mater. Chem.* **2009**, *19*, 1691.

(15) Simão, C.; Mas-Torrent, M.; Crivillers, N.; Lloveras, V.; Artés, J. M.; Gorostiza, P.; Veciana, J.; Rovira, C. *Nat. Chem.* **2011**, *3*, 359.

(16) de Silva, A. P. *Nature* **2008**, *454*, 417.

(17) Gupta, T.; van der Boom, M. E. *Angew. Chem., Int. Ed.* **2008**, *47*, 5322.

(18) Fioravanti, G.; Haraszkiewicz, N.; Kay, E. R.; Mendoza, S. M.; Bruno, C.; Marcaccio, M.; Wiering, P. G.; Paolucci, F.; Rudolf, P.; Brouwer, A. M.; Leigh, D. A. *J. Am. Chem. Soc.* **2008**, *130*, 2593.

(19) Li, H.; Xu, Q. F.; Li, N. J.; Sun, R.; Ge, J. F.; Lu, J. M.; Gu, H. W.; Yan, F. *J. Am. Chem. Soc.* **2010**, *132*, 5542.

(20) Williams, J. M. F., Ferraro, R. J.; Thorn, R. J.; Carlson, K. D.; Geiser, U.; Wang, H. H.; Kini, A. M.; Whangbo, M.-H. *Organic Superconductors (Including Fullerenes): Synthesis, Structure, Properties, and Theory*; Prentice Hall: Englewood Cliffs, NJ, 1992.

(21) Mas-Torrent, M.; Rovira, C. *J. Mater. Chem.* **2006**, *16*, 433.

(22) Batail, P. *Chem. Rev.* **2004**, *104*, 4887.

(23) Farges, J.-F. *Organic Conductors: Fundamentals and Applications*; Marcel Dekker: New York, 1994.

(24) Segura, J. L.; Martín, N. *Angew. Chem., Int. Ed.* **2001**, *40*, 1372.

(25) Hunig, S. *J. Mater. Chem.* **1995**, *5*, 1469.

(26) Herranz, M.; Yu, L.; Martin, N.; Echegoyen, L. *J. Org. Chem.* **2003**, *68*, 8379.

(27) Liu, S. G.; Liu, H.; Bandyopadhyay, K.; Gao, Z.; Echegoyen, L. *J. Org. Chem.* **2000**, *65*, 3292.

(28) Moore, A. J.; Goldenberg, L. M.; Bryce, M. R.; Petty, M. C.; Monkman, A. P.; Marenco, C.; Yarwood, J.; Joyce, M. J.; Port, S. N. *Adv. Mater.* **1998**, *10*, 395.

(29) Herranz, M. A.; Colonna, B.; Echegoyen, L. *Proc. Natl. Acad. Sci. U.S.A.* **2002**, *99*, 5040.

(30) Liu, H. Y.; Liu, S. G.; Echegoyen, L. *Chem. Commun.* **1999**, 1493.

(31) Fujihara, H.; Nakai, H.; Yoshihara, M.; Maeshima, T. *Chem. Commun.* **1999**, 737.

(32) Yokota, Y.; Miyazaki, A.; Fukui, K.; Enoki, T.; Tamada, K.; Hara, M. *J. Phys. Chem. B* **2006**, *110*, 20401.

(33) Canevet, D.; Salle, M.; Zhang, G. X.; Zhang, D. Q.; Zhu, D. B. *Chem. Commun.* **2009**, 2245.

(34) Spencer, H. K.; Cava, M. P.; Garito, A. F. *J. Chem. Soc., Chem. Comm.* **1976**, 966.

(35) Liu, W.; Guo, Y. J.; Zeng, X. R.; Zuo, J. L.; You, X. Z. *J. Heterocycl. Chem.* **2007**, *44*, 831.

(36) Mizuno, M.; Cava, M. P. *J. Org. Chem.* **1978**, *43*, 416.

(37) Otón, F.; Pfattner, R.; Oxtoby, N. S.; Mas-Torrent, M.; Wurst, K.; Fontrodona, X.; Olivier, Y.; Cornil, J.; Veciana, J.; Rovira, C. *J. Org. Chem.* **2011**, *76*, 154.

(38) Hacker, C. A.; Batteas, J. D.; Garno, J. C.; Marquez, M.; Richter, C. A.; Richter, L. J.; Van Zee, R. D.; Zangmeister, C. D. *Langmuir* **2004**, *20*, 6195.

(39) Lee, J.; Jung, B.; Lee, J.; Chu, H.; Dob, L.; Shim, H. *J. Mater. Chem.* **2002**, *12*, 3494.

(40) Blanchard, P.-Y.; Aleveque, O.; Boisard, S.; Gautier, C.; El-Ghayoury, A.; Le Derf, F.; Breton, T.; Levillain, E. *Phys. Chem. Chem. Phys.* **2011**, *13*, 2118.